Structural Chemistry
https://doi.org/10.1007/s11224-024-02341-1

RESEARCH

Crystal structures and Hirshfeld surface analysis of two inner salts of 3-carboxy-2-(quinolinium-1-ylmethyl)propanoate and 3-(3-carbamoylpyridinium-1-yl)-2-(carboxymethyl)propanoate

Yutao Chen[1,2] · Xinyi Hong[1,2] · Shouwen Jin[1,2] · Xiaodan Ma[1,2] · Yanglin Ji[1,2] · Xusen Gong[1,2] · Ronghui Wu[2] · Daqi Wang[3]

Received: 29 April 2024 / Accepted: 10 May 2024

Abstract
Two crystalline inner salts 3-carboxy-2-(quinolinium-1-ylmethyl)propanoate dihydrate **(1)** and 3-(3-carbamoylpyridinium-1-yl)-2-(carboxymethyl)propanoate **(2)** were featured by the X-ray diffraction analysis, IR, mp, and elemental analysis. Salt **1** crystallizes in the triclinic, space group P-1, with $a = 7.8315(8)$ Å, $b = 11.1063(12)$ Å, $c = 11.3763(14)$ Å, $\alpha = 67.5800(10)°$, $\beta = 82.295(2)°$, $\gamma = 80.970(2)°$, $V = 900.38(17)$ Å^3, and $Z = 2$. Salt **2** adopts the monoclinic, space group P2(1)/*n*, with $a = 8.4782(8)$ Å, $b = 7.7825(7)$ Å, $c = 16.8649(17)$ Å, $\beta = 97.999(2)°$, $V = 1101.95(18)$ Å^3, and $Z = 4$. Both salts comprise the extensive O-H···O H-bonds as well as other non-covalent associates. The percentage contribution of the significant non-covalent contacts was calculated *via* the Hirshfeld surface analysis. The hetero supramolecular synthons $R_2^1(6)$, $R_2^2(10)$, $R_2^2(12)$, $R_2^2(13)$, $R_2^2(14)$, $R_2^2(16)$, $R_2^2(22)$, $R_3^3(9)$, $R_4^2(8)$, $R_4^3(10)$, and $R_5^5(17)$ were established at the both salts. Most of the synthons were not found repeatedly, yet the $R_2^2(10)$ was established in both cases. The role of these non-covalent interactions in the crystal structure extension is ascertained. These weak interactions combined together, and both salts exhibited the 3D framework structures.

Keywords Crystal structures · Hydrogen bonding · Non-covalent interactions · Hirshfeld surface analysis · Inner salts

Introduction

Crystallization is frequently considered as an art. Notwithstanding, even a highly skilled artist in this area often finds it difficult, sometimes even impossible to get a diffraction-quality single crystal. The major obstacle could be attributed to the fact that although the process of crystallization has been studied historically, the inner theory of the crystallization process/crystal growth, at the molecular level, is still a murkier subject [1, 2]. Even with the advent of highly sophisticated instruments and popular theory, there still exists a long way off from predicting the outcome of a crystallization process accurately at the molecular level. Instead, the popular crystallization theories are usually based on the crystal engineering theory with the background of chemical and physical knowledge to create the supramolecular structures from molecules that are programmed to participate in the multiple interactions of electrostatic forces, H-bonding, cation···π interaction, CH-π, and π···π interactions [3–8]. H-bonding is one of the most critical non-covalent associates that determine and control the assembly of the molecules and ions [9–12]. In recent years, efforts have been made to explore the construction of supermolecules or supramolecular arrays utilizing non-covalent bonding. Thus, the supramolecular construction successfully exploits the hydrogen bonding and other types of non-covalent interactions in creating the supramolecular systems [13]. In this regard, there are many interesting topological structures such as one-dimensional (1-D) tapes, two-dimensional (2-D) sheets, and

1Xinyi Hong, and Xiaodan Ma equally contributed to this work as Yutao Chen, and they are all the first authors.

✉ Shouwen Jin
jinsw@zafu.edu.cn

[1] Jiyang college ZheJiang A & F University, Zhu'ji, Zhejiang Province 311800, China

[2] Key Laboratory of Chemical Utilization of Forestry Biomass of Zhejia ng Province Zhejiang A & F University, Lin'an, Zhejiang Province 311300, P. R. China

[3] Department of Chemistry, Liaocheng University, Liaocheng 252059, P. R. China

Published online: 08 June 2024

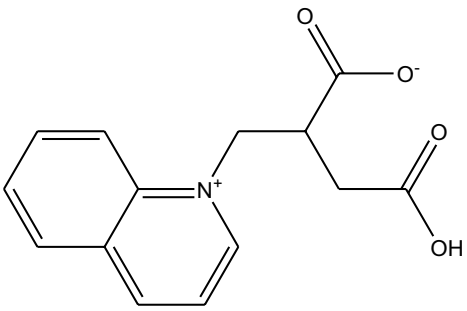

3-carboxy-2-(quinolinium-1-ylmethyl)propanoate

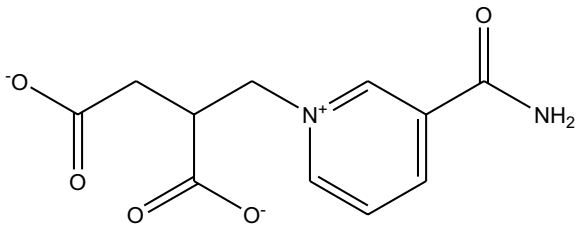

3-(3-carbamoylpyridinium-1-yl)-2-(carboxymethyl)propanoate

Scheme 1 The inner salts discussed in this paper

three-dimensional (3-D) networks which have been built by the H-bonding associates [14, 15].

In zwitterionic compounds, oppositely charged quaternary ammonium groups are connected with the necked carboxylate group *via* the methylene groups [16–20], and they are also known as betaines. Another group of betaines is the heterocyclic betaines, and the most common heterocyclic unit is the pyridine ring. Although some betaines with pyridine units have been documented [21–26], there were very few inter salts with the quinoline and nicotinamide moiety, especially concerning the (carboxymethyl)propanoate simultaneously.

Therefore, it is essential to study the supramolecular interactions of the inter salts derived from quinoline and nicotinamide; herein, we unveil the structures of the two inner salts derived from quinoline and nicotinamide (Scheme 1), respectively. The two organic inner salts are 3-carboxy-2-(quinolinium-1-ylmethyl)propanoate dihydrate **(1)** and 3-(3-carbamoylpyridinium-1-yl)-2-(carboxymethyl)propanoate **(2)**, and the synthons in them were compiled in Scheme 2 (Scheme 2). The characterization of the inner salts was performed using the following techniques: single-crystal X-ray diffraction (SCXRD), elemental analysis (EA), and melting point measurement.

Experimental section

Materials and physical measurements

The chemicals and solvents used in this job are of analytical grade and available commercially and were utilized without further purification. The FT-IR spectra were recorded from the KBr pellets in the range 4000–400 cm^{-1} on a Mattson Alpha-Centauri device. Microanalytical (C, H, and N) data were registered with a Perkin-Elmer Model 2400II elemental analyzer. Melting points of the inner salts were recorded on an XT-4 thermal apparatus without correction.

Crystal growth of the inner salts 1–2

3-carboxy-2-(quinolinium-1-ylmethyl)propanoate dihydrate (1)

3-Carboxy-2-(quinolinium-1-ylmethyl)propanoate (25.9 mg and 0.1 mmol) was dissolved in methanol (10 mL). The solution was stirred for a few minutes; then, the solution was filtered into a test tube. The solution was left standing at room temperature for several days, and colorless block crystals were isolated after slow evaporation of the methanol solution in the air. The crystals were collected and dried in air to give the title compound 3-carboxy-2-(quinolinium-1-ylmethyl)propanoate dihydrate (**1**). (yield 22.4 mg, 75.86%). mp 159–161 °C. Elemental analysis: Calc. for $C_{14}H_{17}NO_6$ (295.28): C, 56.89; H, 5.76; N, 4.74. Found: C, 56.85; H, 5.72; N, 4.71. Infrared spectrum (cm^{-1}): 3721 s(br, ν(OH), 3268 s(ν_{as}(NH)), 3152 s(ν_s(NH)), 3066 m, 3023 m, 2971 m, 2932 m, 1657 s(ν_{as}(C = O)), 1616 s(ν_{as}(COO^-)), 1570 m, 1528 m, 1480 m, 1430 m, 1386 s(ν_s(COO^-)), 1344 m, 1304 m, 1286 s(ν_s(C-O)), 1242 m, 1200 m, 1159 m, 1115 m, 1072 m, 1030 w, 988 w, 946 m, 905 m, 861 m, 818 m, 777 w, 732 m, 690 m, 651 w, 634 m, and 604 m.

3-(3-carbamoylpyridinium-1-yl)-2-(carboxymethyl) propanoate (2)

3-(3-carbamoylpyridinium-1-yl)-2-(carboxymethyl)propanoate (25.2 mg and 0.1 mmol) was dissolved in methanol (12 mL). The solution was stirred for a few minutes; then, the solution was filtered into a test tube. The solution was left standing at room temperature for several days, and colorless block crystals were isolated after slow evaporation of the methanol solution in air. The crystals

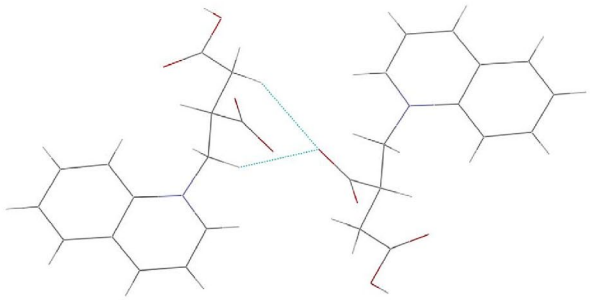

I $R_2^1(6)$

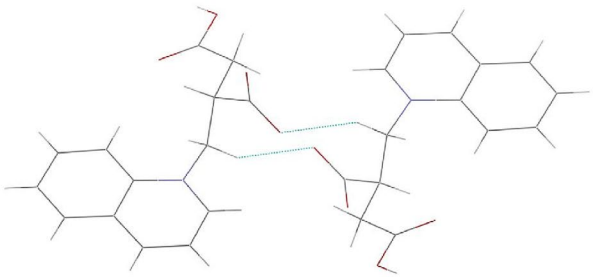

II $R_2^2(10)$

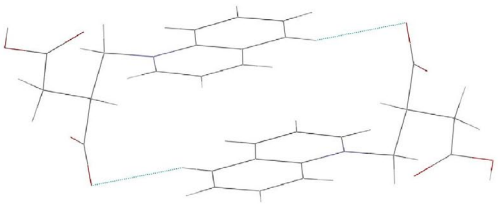

III $R_2^2(22)$

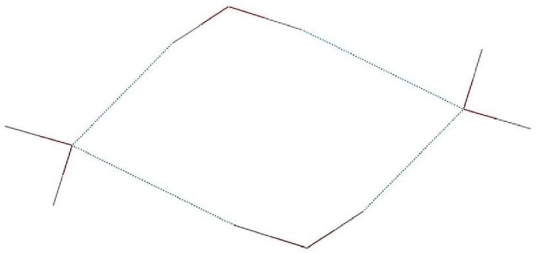

IV $R_4^2(8)$

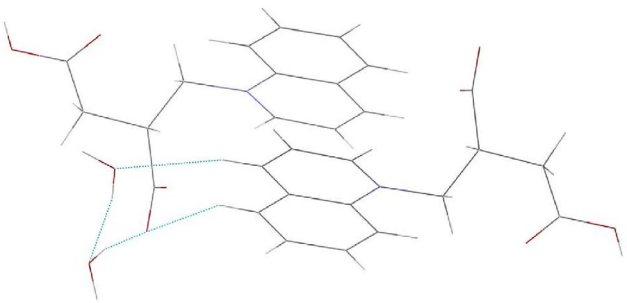

V $R_4^3(10)$

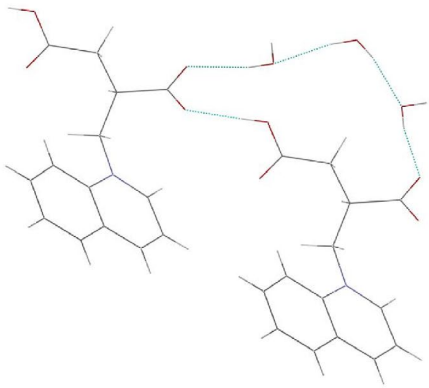

VI $R_5^5(17)$

Scheme 2 The synthons in **1**-**2**

were collected and dried in air to give the title compound 3-(3-carbamoylpyridinium-1-yl)-2-(carboxymethyl)propanoate **(2)**. (yield: 20 mg, 79.29%). mp 187–189 °C. Elemental analysis: Calc. for $C_{11}H_{12}N_2O_5$ (252.23): C, 52.33; H, 4.76; N, 11.10. Found: C, 52.28; H, 4.72; N, 11.06. Infrared spectrum (cm^{-1}): 3648 s(ν(OH)), 3230 s(ν_{as}(NH)), 3166 s(ν_s(NH)), 3074 m, 2982 m, 2936 m, 2855 m, 1708 s(ν(C = O)), 1644 s, 1599 s(ν_{as}(COO^-)), 1556 m, 1519 m, 1472 m, 1428 m, 1384 s(ν_s(COO^-)), 1324 s(νs(NO_2)), 1288 s(ν(C-O)), 1245 m, 1201 m, 1158 m, 1115 m, 1071 m, 1028 m, 987 m, 945 m, 903 m, 858 m, 812 m, 768 m, 726 m, 684 m, 649 m, and 614 m.

X-ray crystallography and data collection

Suitable crystals were mounted on a glass fiber by a Bruker SMART 1000 CCD diffractometer operating at 50 kV and 40 mA power using the Mo Kα radiation (0.71073 Å) with the CCD area detector. Data were collected using the φ and ω scans at 0.9° and 15 s exposures per frame. Data collection and reduction were performed by the utilization of the SMART and SAINT software [27]. The structures were solved by the direct methods, and the non-hydrogen atoms were subjected to anisotropic refinement by the full-matrix least squares against F^2 employing the SHELXTL

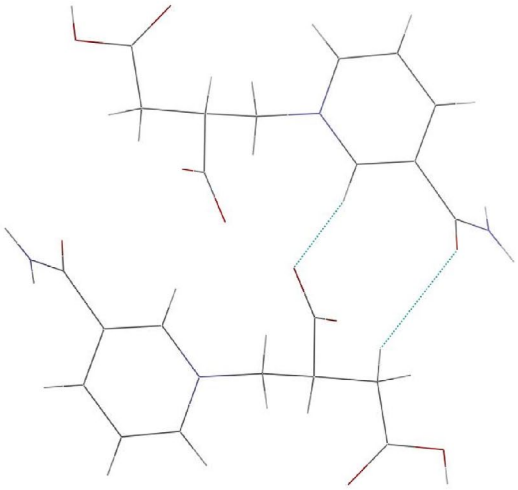

VII $R_2^2(10)$

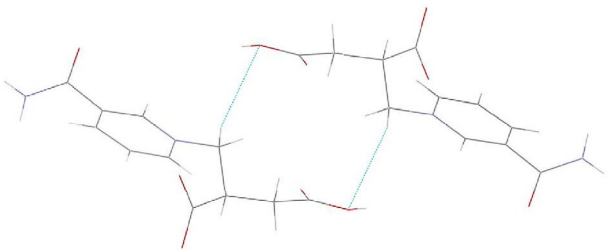

VIII $R_2^2(12)$

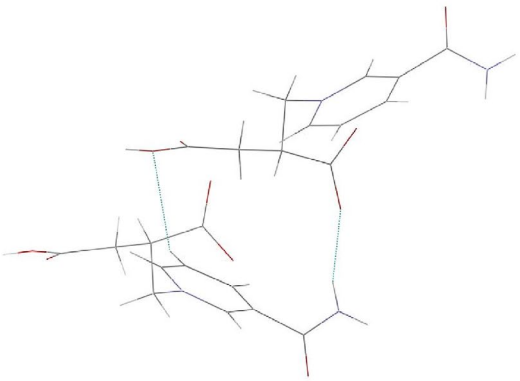

IX $R_2^2(13)$

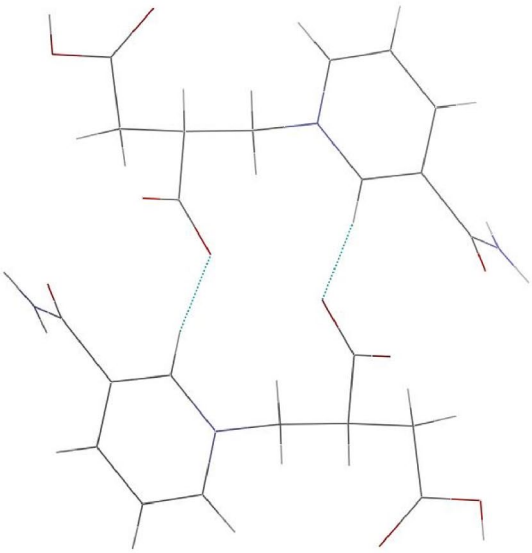

X $R_2^2(14)$

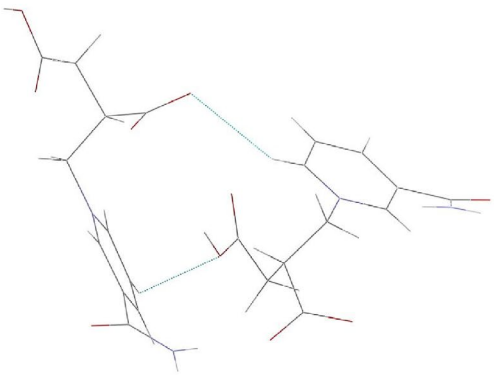

XI $R_2^2(16)$

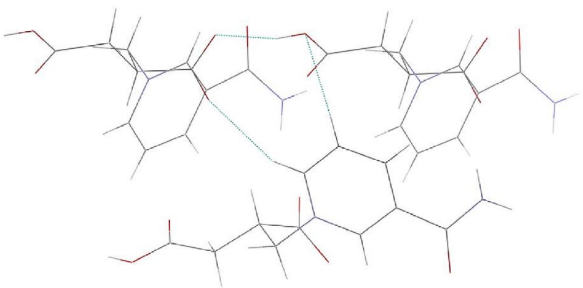

XII $R_3^3(9)$

Scheme 2 (continued)

package [28]. The hydrogen atoms anchored to the carbon atoms were ridden at the geometrically calculated sites with C-H = 0.93 Å (aryl), and C-H = 0.97–0.98 Å (for the sp^3 C atoms), the hydrogen atoms tied to the nitrogen and oxygen atoms were located on a Fourier difference map and refined without AFIX command, with Uiso(H) = 1.2Ueq(C, N) and Uiso(H) = 1.5 Ueq(O). Further details of the structural analysis are summarized in Table 1. Selected bond lengths and angles for the salts **1**–**2** are listed in Table 2, and the relevant hydrogen bond parameters are provided in Table 3.

Results and discussion

Preparation and general characterization

The crystals **1**–**2** were grown by evaporating the methanol solution at ambient conditions. Both structures are inner salts showing no hygroscopic. The molecular structures and their atom labeling schemes for the both structures are demonstrated in Figs. 1 and 2, respectively. The elemental analysis data for the both crystalline inner salts are in good alignment with their compositions. The infrared spectra of both compounds are consistent with their chemical formulas measured by the elemental analysis and further confirmed by the X-ray diffraction analysis.

The very strong and broad features at approximately 3152–3721 cm^{-1} in the IR spectra of both inner salts arise from the O-H or N-H stretching frequencies. Aryl ring (including the pyridine and the quinoline) stretching and bending are connected with the medium intensity bands in the regions of 1500–1630 and 600–750 cm^{-1}, respectively. The inner salts **1**–**2** exhibit the characteristic bands for the CO_2H groups. IR spectroscopy has also been proven to be useful for the detection of the CO_2^- groups [29, 30].

Table 1 Summary of X-ray crystallographic data for compounds **1–2**

	1	**2**
Formula	$C_{14}H_{17}NO_6$	$C_{11}H_{12}N_2O_5$
Fw	295.29	252.23
T, K	298(2)	298(2)
Wavelength, Å	0.71073	0.71073
Crystal system	Triclinic	Monoclinic
Space group	P-1	P2(1)/*n*
a, Å	7.8315(8)	8.4782(8)
b, Å	11.1063(12)	7.7825(7)
c, Å	11.3763(14)	16.8649(17)
α, deg.	67.5800(10)	90
β, deg.	82.295(2)	97.999(2)
γ, deg.	80.970(2)	90
V, $Å^3$	900.38(17)	1101.95(18)
Z	2	4
D_{calcd}, Mg/m^3	1.089	1.520
Absorption coefficient, mm^{-1}	0.086	0.122
F(000)	312	528
Crystal size, mm^3	0.50 × 0.18 × 0.13	0.27 × 0.21 × 0.10
θ range, deg	3.12–25.02	2.86–25.02
Limiting indices	$-9 \le h \le 6$ $-13 \le k \le 13$ $-13 \le l \le 13$	$-10 \le h \le 9$ $-7 \le k \le 9$ $-19 \le l \le 20$
Reflections collected	4560	5189
Reflections independent (R_{int})	3143 (0.0321)	1943 (0.0851)
Goodness-of-fit on F^2	0.867	1.032
R indices [$I > 2\sigma I$]	0.0849, 0.2293	0.0723, 0.1801
R indices (all data)	0.1461, 0.2609	0.1305, 0.2272
Largest diff. peak and hole, e.$Å^{-3}$	0.423, −0.295	0.493, −0.251

Table 2 Selected bond lengths [Å] and angles [°] for **1–2**

1			
N(1)-C(6)	1.317(5)	N(1)-C(10)	1.409(5)
N(1)-C(5)	1.480(5)	O(1)-C(1)	1.247(4)
O(2)-C(1)	1.234(4)	O(3)-C(4)	1.302(5)
O(4)-C(4)	1.206(5)	C(6)-N(1)-C(10)	120.3(4)
C(6)-N(1)-C(5)	118.5(3)	C(10)-N(1)-C(5)	121.3(4)
O(2)-C(1)-O(1)	124.9(3)	O(4)-C(4)-O(3)	124.0(4)
2			
N(1)-C(11)	1.341(5)	N(1)-C(7)	1.342(5)
N(1)-C(5)	1.482(5)	N(2)-C(6)	1.313(5)
O(1)-C(1)	1.260(5)	O(2)-C(1)	1.241(5)
O(3)-C(4)	1.283(5)	O(4)-C(4)	1.206(6)
O(5)-C(6)	1.228(5)	C(11)-N(1)-C(7)	120.9(4)
C(11)-N(1)-C(5)	119.0(4)	C(7)-N(1)-C(5)	120.1(4)
O(2)-C(1)-O(1)	125.0(4)	O(4)-C(4)-O(3)	123.8(4)
O(5)-C(6)-N(2)	125.3(4)		

Structural descriptions

X-ray structure of 3-carboxy-2-(quinolinium-1-ylmethyl) propanoate dihydrate (1)

The crystal structure of the inner salt **1** consists of one 3-carboxy-2-(quinolinium-1-ylmethyl)propanoate and two water molecules in the asymmetric unit (ASU) (Fig. 1). The inner salt **1** crystallizes in the triclinic space group P-1 with one CO_2H group ionized, and the other CO_2H group remains protonized.

The C-O bond lengths 1.240(3) Å (O(2)-C(1)) and 1.249(3) Å (O(1)-C(1)) concerning the carboxylate are within the range of the deprotonated CO_2H unit [31]. In the CO_2H group, the two C-O bond lengths are obviously different between O(3)-C(4) (1.299(4) Å) and O(4)-C(4) (1.204(4) Å) with the large Δ value of 0.095 Å. The

Table 3 Hydrogen bond distances and angles in studied structures 1–3

D-H···A	d(D-H) [Å]	d(H···A) [Å]	d(D···A) [Å]	< (DHA)[°]
		1		
O(6)-H(6D)···O(5)#1	0.85	2.11	2.945(6)	168.9
O(6)-H(6 C)···O(5)	0.85	1.99	2.825(5)	168.2
O(5)-H(5 F)···O(2)#1	0.85	1.95	2.784(4)	169.1
O(5)-H(5E)···O(2)#2	0.85	1.98	2.818(4)	169.2
O(3)-H(3)···O(1)#2	0.82	1.72	2.535(4)	171.4
		2		
O(3)-H(3)···O(1)#1	0.82	1.68	2.481(4)	166.3
N(2)-H(2B)···O(2)#2	0.86	2.02	2.848(5)	161.6
N(2)-H(2 A)···O(5)#3	0.86	2.05	2.898(5)	169.0

Symmetry transformations used to generate equivalent atoms for **1**: #1 -x+1, -y+1, -z+1; #2 x-1, y, z. Symmetry transformations used to generate equivalent atoms for **2**: #1 x, y+1, z; #2 -x+1/2, y-1/2, -z+3/2; #3 -x, -y-1, -z+2

relatively large Δ value which is expected for the neutral C = O and C-O bonds [32] are also corroborating the reliability of adding the H atoms experimentally by the different electron densities onto the O atoms (Table 3). Quaternization of the quinoline at the cyclic N1 site is reflected in a change in the bond angle. The angle at the unquaternizated ring atom is ca. 118 ° [33], while around the quaternizated N, the angle (C(6)-N(1)-C(10)) is 120.2(3)°. The rms deviation of the quinoline plane is 0.0108 Å, the C1-O1-O2/C4-O3-O4 inclined at 86.8/24.2° from the quinoline plane. Both planes defined by the COO^{-}/COOH groups in the same inner salt were almost perpendicular to each other with a dihedral angle of 90.6°.

Two water molecules produced a water dimer *via* the O-H···O hydrogen bond with the O···O = 2.825(5) Å. At the 3-carboxy-2-(quinolinium-1-ylmethyl)propanoate, there adhered a water dimer by the CH-O associate present between the 4-CH(C8H8) of the quinoline and the O(O6) atom of one water molecule at the water dimer with C···O = 3.408(2) Å/< CHO = 166(4)° to attain a tri-component aggregate. Both tri-component aggregates were held together by the O(5)-H(5F)···O(2)#1 hydrogen bond donated by the water molecule to one O atom of the carboxylate with O···O = 2.775(4) Å, and CH-O association operated between the 5-CH(C14H14) of the quinoline and the same O(O2) atom of the carboxylate that

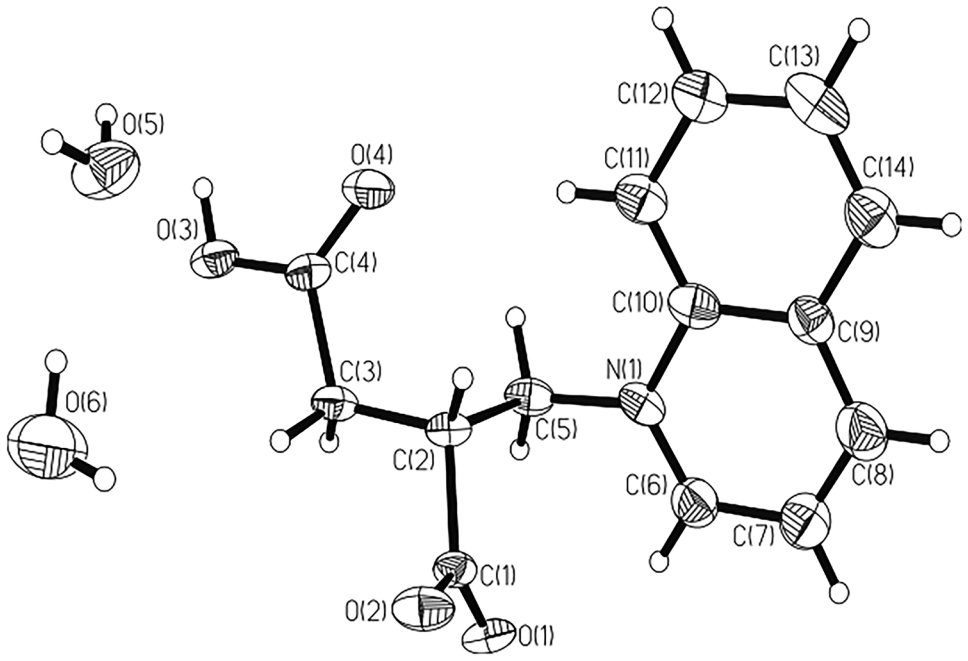

Fig. 1 Molecular structure of **1** showing the atomic numbering scheme. Displacement ellipsoids are drawn at the 30% probability level

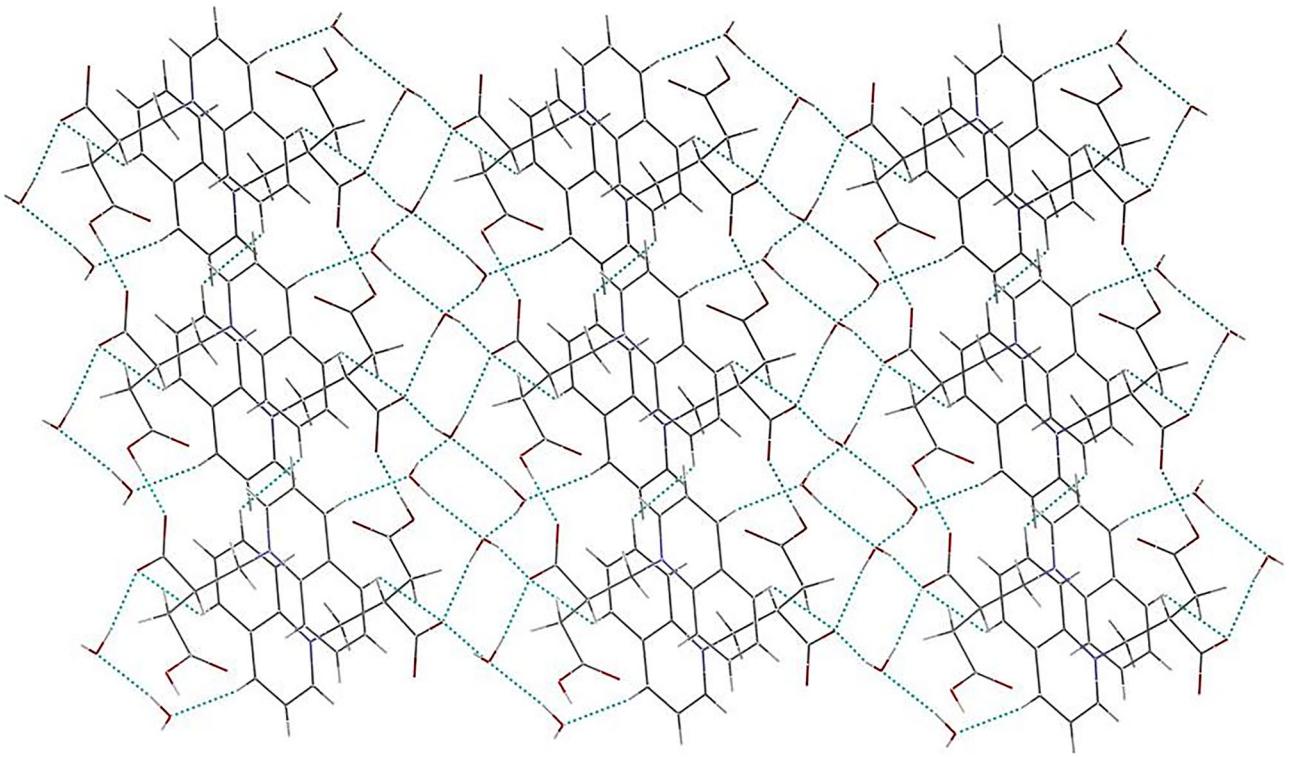

Fig. 2 Molecular structure of **2** showing the atomic numbering scheme. Displacement ellipsoids are drawn at the 30% probability level

was involved in the O-H···O H-bond with C···O = 3.355(4) Å< CHO = 128(3)° to create a six-component assembly. The geometries of the CH-O associates were in the limit of the report [34]. Both tri-component aggregates at the six-component assembly were inversionally related. The six-component assemblies were interlinked by the O(3)-H(3)···O(1)#2 H-bond generated between the CO_2H and the CO_2^- with O···O separation = 2.530(3) Å to get the 1D chain extending along the crystallographic *a* axis direction; here, the O···O separation was ca. 0.1 Å shorter than the document with the $CO_2H\cdots CO_2^-$ associate [35]. The 1D chains were fused together by the O(5)-H(5E)···O(2)#2 hydrogen bond operated between the water molecule and the carboxylate with O···O = 2.818(3) Å to reach 2D sheet

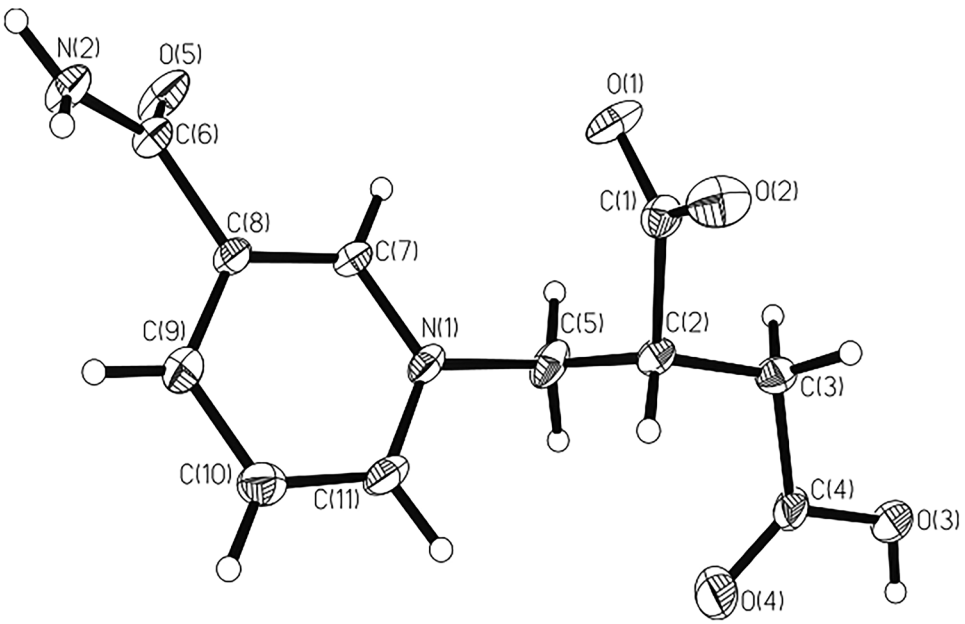

Fig. 3 2D sheet structure of 1 extending parallel to the ac crystallographic plane

extending parallel to the crystallographic *ac* plane (Fig. 3). The 2D sheets were further piled at the crystallographic *b* axis direction by the CH_2-O associate present between the CH_2(C5H5A and C3H3A) spacer of the 3-carboxy-2-(quinolinium-1-ylmethyl)propanoate and the oxygen atom (O1) in the carboxylate with C···O amounting to 3.437(4)–3.595(4) Å and the < CHO = 148(4)/153(4)° to create the 3D network structure. The geometries of the CH_2-O associates were close to the document [36]. The I $R_2^1(6)$, II $R_2^2(10)$, III $R_2^2(22)$, IV $R_4^2(8)$, V $R_4^3(10)$, and VI $R_5^5(17)$ graph sets were established in the net.

X-ray structure of 3-(3-carbamoylpyridinium-1-yl) -2-(carboxymethyl)propanoate (2)

As **1**, the crystal of **2** was also grown by slow evaporation of its CH_3OH solution, comprising only one 3-(3-carbamoylpyridinium-1-yl)-2-(carboxymethyl) propanoate in its ASU (Fig. 2). The compound **2** is also an inner salt, in which only one proton of the two carboxyl groups was ionized. It adopts the monoclinic space group P2(1)/*n*. The C-O bond length of the O(5)–C(6) (1.228(5) Å) is of the common C = O double bond. Quaternization of the nicotinamide on the N1 site is reflected in a change in the bond angle. The angle at the unquaternizated ring N atom is 118.56(13)° [37], while for the quaternizated N, the angle (C(11)–N(1)-C(7)) is 120.5(4)°. And this angle also resembled that found in **1**. The nicotinamide moiety adopted the E conformation according to Fausto [38], in which the O(5)-C(6)-C(8)-C(9) torsion angle is −134.7(5)°. The rms deviation of the pyridine ring N1-C7–C11 was 0.0101 Å, the C1-O1-O2/C4-O3-O4 inclined at 94.7(2)/37.6(2)° from the pyridine plane. Both planes defined by the COO^-/COOH groups in the same inner salt were almost perpendicular to

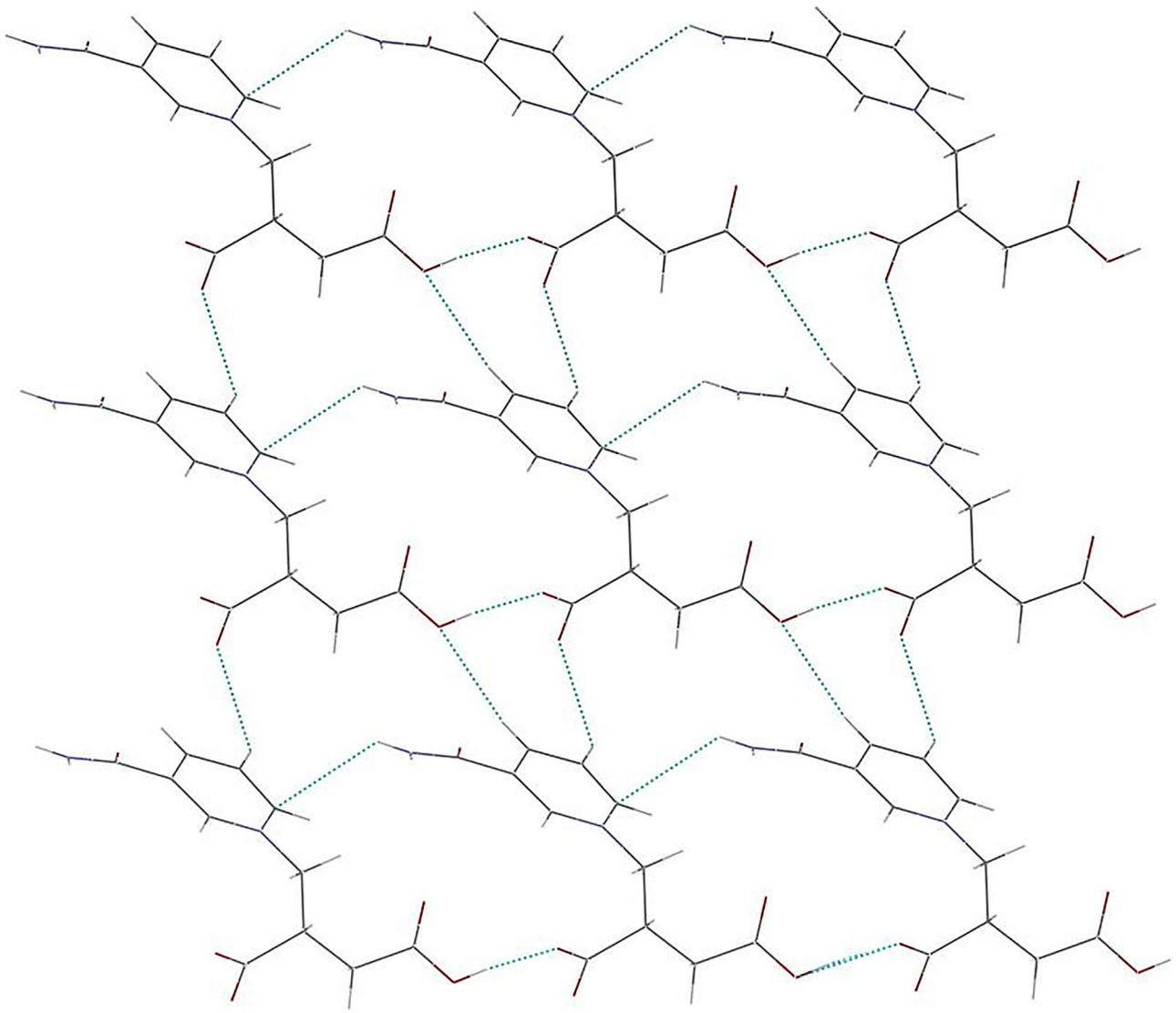

Fig. 4 2D sheet structure of 2 extending parallel to the ab crystallographic plane

each other with a dihedral angle of 83.6(2)°. The $CONH_2$ deviated by 137.7(2)° from the pyridine plane.

The 3-(3-carbamoylpyridinium-1-yl)-2-(carboxymethyl) propanoates were linked together by the O(3)-H(3)···O(1)#3 hydrogen bond of the COOH···COO^- mode with O···O distance of 2.481(4) Å, and NH-π associate operated between the NH_2 of the nicotinamide fragment and the pyridine kernel with N···Cg = 3.352(2) Å to get the 1D chain stretching along the crystallographic *b* axis direction. The COOH···COO^- hydrogen bond parameters were close to that at **1**. In this case, the N···Cg distance is in the limit of the reported values [39]. The 1D chains were tethered together by the CH-O association stemmed from the 4-CH(C9H9) of the nicotinamide residue and the OH(O3) at the CO_2H with C···O = 3.439(3) Å and < CHO = 143(4)° and CH-O associate between the 5-CH(C10H10) of the nicotinamide residue and the O(O2) atom at the CO_2^- with C···O = 3.245(2) Å and < CHO = 123(2)° to get 2D sheet spreading parallel to the crystallographic *ab* plane (Fig. 4). The 2D sheets were further packed along the crystallographic *c* axis direction through the N(2)-H(2B)···O(2)#2 hydrogen bond established between the NH_2 of the nicotinamide residue and

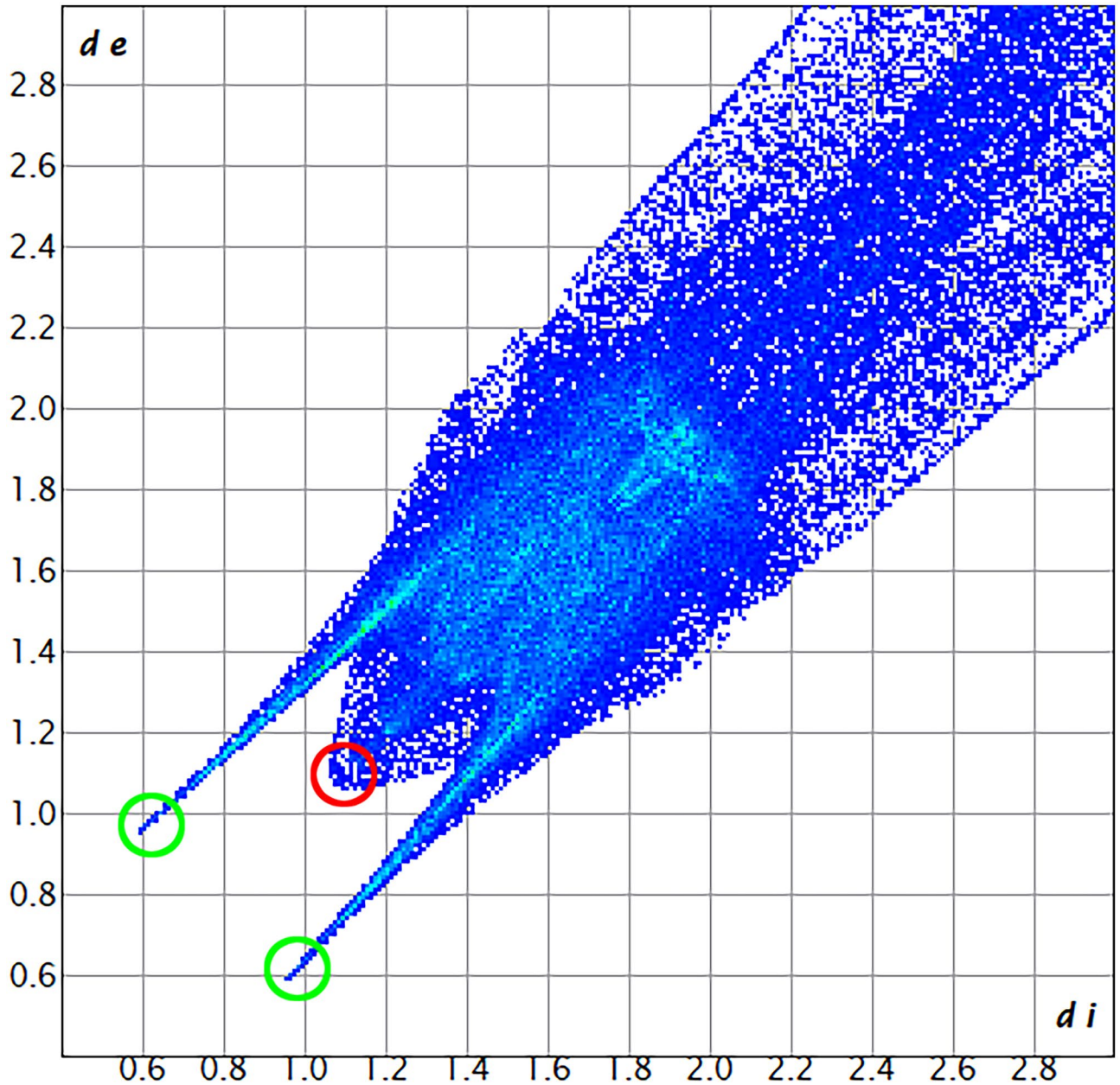

Fig. 5 Fingerprint plots computed from Hirshfeld surfaces of **1**. H···H contacts are highlighted in red circle, and H···O contacts are highlighted in green circle

the CO_2^- with N···O = 2.842(5) Å, CH-O association present between the 5-CH(C10H10) of the nicotinamide and the OH(O3) at the carboxyl with C···O = 3.335(2) Å and < CHO = 125(2)°, and CH-O association operated between the 6-CH(C11H11) of the nicotinamide and the O(O2) at the CO_2^- with C···O = 3.442(2) Å and < CHO = 145(2)° to make the 3D layer network structure. The N···O separation at the N-H···O hydrogen bond is considerably less than the sum of the van der Waals radii for the N and O (3.07 Å) atoms [40]. The geometries of the CH-O associations resembled those at **1** too. There established the VII $R_2^2(10)$, VIII $R_2^2(12)$, IX $R_2^2(13)$, X $R_2^2(14)$, XI $R_2^2(16)$, and XII $R_3^3(9)$ synthons.

The Hirshfeld surface analysis

The Hirshfeld surfaces and fingerprint plots were generated from the CIF files of the respective inner salts utilizing the Crystal Explorer (Version 21.5) suite. Hirshfeld surfaces [41] and related fingerprint plots [42, 43] were calculated for each compound (Figs. 5 and 6),

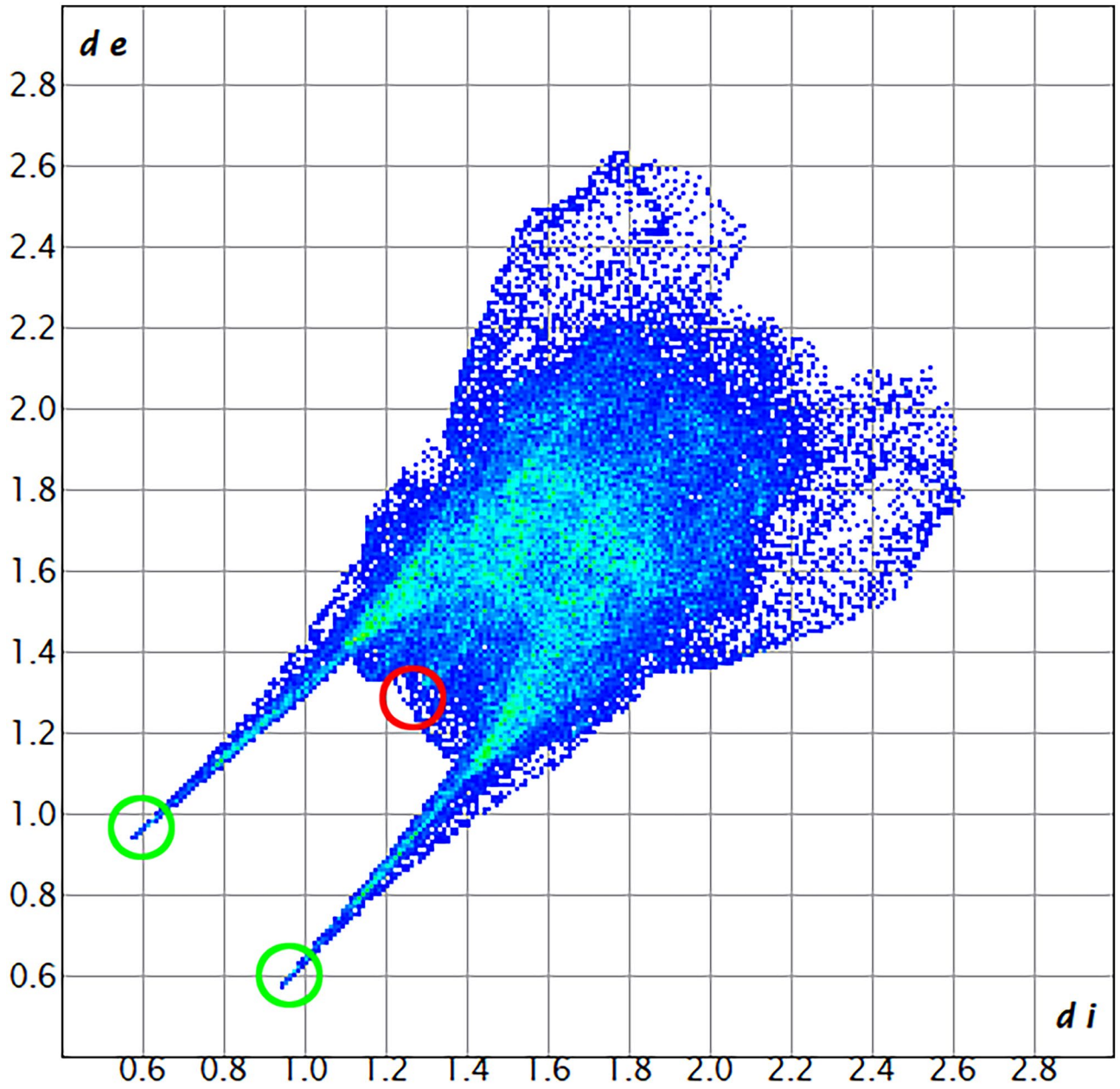

Fig. 6 Fingerprint plots computed from Hirshfeld surfaces of **2**. H···H contacts are highlighted in red circle, and H···O contacts are highlighted in green circle

Table 4 Summary of the various contact contributions to the Hirshfeld surface area in **1**–**2**

Contact	**1**	**2**
H···H	50.8%	30.0%
H···O	34.9%	47.4%
H···C	5.7%	8.8%
H···N	0.2%	1.1%
N···O		2.8%
N···C	0.2%	0.1%
C···C	3.2%	1.5%
C···O	4.7%	7.9%
O···O	0.3%	0.4%

and the percentage contribution of the significant non-covalent contacts at each inner salt is compiled in Table 4. The H···H interactions in **1** and **2** occupy 50.8% and 30.0% of the total Hirshfeld surfaces at **1** and **2**. The The H···O interactions occupy 34.9% and 47.4% of all Hirshfeld surfaces for **1**–**2**, respectively. **1** has the biggest percent of the H···H interaction for it bears more H atoms than **2**. The H···O interaction at **2** has the largest percent because there existed more CH-O contacts, which is also supported by the relative high C···O contact at **2**. The H···C interaction composes 5.7% and 8.8% of the total Hirshfeld surfaces at **1**–**2**, respectively.

Conclusions

In summary, 2 quinolinium/pyridinium (carboxymethyl) propanoate inner salts have been structurally featured and the underlying supramolecular chemistry has been elucidated in this article, which make new knowledge into the inner salt motifs. In both the inner salts, the cyclic ring N is quaternized. In this report, a complex sets of synthons with small and large circles were made as $R_2^1(6)$, $R_2^2(10)$, $R_2^2(12)$, $R_2^2(13)$, $R_2^2(14)$, $R_2^2(16)$, $R_2^2(22)$, $R_3^3(9)$, $R_4^2(8)$, $R_4^3(10)$, and $R_5^5(17)$. Major of the synthons were not found repeatedly, yet the $R_2^2(10)$ appeared at both **1** and **2**.

Though prepared *via* the same natural solvent evaporation technique, they both showed the 3D net motifs. All bear the 2D sheet substructure, and there also built the subchain at both; it seems that the intra- and interchain non-covalent bonds showed equal merit in the structure propagation. Despite variations in the aryl cores, Both established the strong intermolecular O-H···O H-bonds. Hirshfeld surface analysis discloses that the H···H/H···O intermolecular interactions act as the influential parts to ascertain the crystal packing arrangements. Apart from the robust classical H-bonds, other different sets of the supramolecular associates of CH-O, CH_2-O, and NH-π are also crucial in structure expansion. The CH-O contacts were created in both the salts. The various non-covalent bonds coupled with the different functional groups at the quinoline/pyridine resulted in the construction of the higher-dimensional assemblies from the discrete blocks. Based on the inner salts discussed here as well as those from the literatures, the results clearly tell that the quinoline/pyridine is a good segment to be built into the inner salts so as to get the diversiform and stable H-bonded systems.

Supplementary Information The online version contains supplementary material available at https://doi.org/10.1007/s11224-024-02341-1.

Author contribution Yutao Chen, Xinyi Hong, Xiaodan Ma, and Shouwen Jin performed the synthesis experiments and drew the figures. Yanglin Ji and Xusen Gong performed the MP and gave some suggestions for the writing. Shouwen Jin wrote the main manuscript, and Ronghui Wu interpreted the data and made some checks on the text. Daqi Wang performed the XRD and solved the single crystal data. All authors reviewed the manuscript.

Funding This research was supported by Zhejiang Provincial Natural Science Foundation of China under Grant No. LY14B010006, Jiyang 533 project RC2022F01 for Shouwen Jin, the National Training Programs of Innovation and Entrepreneurship of China for Undergraduates and the Jiyang college Programs of Innovation and Entrepreneurship for Xinyi hong for Undergraduates.

Data availability No datasets were generated or analyzed during the current study.

Declarations

Ethical approval Not applicable.

Competing interests The authors declare no competing interests.

References

1. Hollingworth MD (2002) Crystal engineering: From structure to function. Science 295:2410–2413
2. Mullin JW (1993) Crystallization, 3rd edn. Heinemann-Butterworth, London
3. Steiner T (2002) The hydrogen bond in the solid state. Angew Chem Int Ed 41:48–76
4. Ma JC, Dougherty DA (1997) The cation−π interaction. Chem Rev 97:1303–1324
5. Nishio M (2004) CH/π hydrogen bonds in crystals. CrystEngComm 6:130–158
6. Claessens CG, Stoddart JF (1997) π–π Interactions in self-assembly. J Phys Org Chem 10:254–272
7. Meyer EA, Castellano RK, Diederich F (2003) Interactions with aromatic rings in chemical and biological recognition. Angew Chem Int Ed 42:1210–1250
8. Desiraju GR (1995) Supramolecular synthons in crystal engineering—a new organic synthesis. Angew Chem Int Ed 34:2311–2327
9. Desiraju GR (2002) Hydrogen bridges in crystal engineering: Interactions without borders. Acc Chem Res 35:565–573
10. Braga D, Maini L, Paganelli F, Tagliavini E, Casolari S, Grepioni F (2001) Organometallic building blocks for crystal engineering. Synthesis, structure and hydrogen bonding interactions in [Fe(η^5-$C_5H_4CH_2(CH_3)OH)_2$], [Fe(η^5-$C_5H_3(CH_3)COOH)_2$], [Fe(η^5-$C_5H_4CH(CH_3)NH(\eta^5$-$C_5H_4CH(CH_3))$] and in the diaminecyclohexane

salt $[Fe(\eta^5\text{-}C_5H_4COO)2]^{2-}[(1S,2S)\text{-}(NH_3)_2C_6H_{10}]^{2+}\cdot 2[H_2O]$. J Organomet Chem 637:609–615
11. Liu JQ, Wang YY, Ma LF, Zhang WH, Zeng XR, Zhong F, Shi QZ, Peng SM (2008) Three new supramolecular networks formed via hydrogen bonding interactions: syntheses, crystal structures and magnetic properties. Inorg Chim Acta 361:173–182
12. Biswas C, Drew MGB, Escudero D, Frontera A, Ghosh A (2009) Anion–π, Lone-Pair–π, π–π and hydrogen-bonding interactions in a Cu^{II} complex of 2-Picolinate and protonated 4,4′-Bipyridine: Crystal structure and theoretical studies. Eur J Inorg Chem 2238–2246
13. Maamen M, Gordon DM (1995) Noncovalent synthesis: using physical-organic chemistry to make aggregates. Acc Chem Res 28:37–44
14. Weyna DR, Shattock T, Vishweshwar P, Zaworotko MJ (2009) Synthesis and structural characterization of cocrystals and pharmaceutical cocrystals: Mechanochemistry vs slow evaporation from solution. Cryst Growth Des 9:1106–1123
15. Du M, Zhang ZH, Zhao XJ (2005) Cocrystallization of trimesic acid and pyromellitic acid with bent dipyridines. Cryst Growth Des 5:1247–1254
16. Alcalde E, Gisbert M, Perez-Garcia L (1996) Heterocyclic Betaines. XXIII. Access to novel dipolar ethyleneimidazolium(pyridinium) 4-nitrobenzimidazolate inner salts. Synthesis, characterization and reactivity concerning a type of β-elimination reaction. Chem Pharm Bull 44:29–33
17. Alcalde E, Gisbert M, Perez-Garcia L, Dinares I, Frigola J (1991) An efficient synthesis of 2-vinylbenzimidazoles from 1-(2-(benzimidazol-2-ylethyl) pyridinium salts using an anion-exchange resin. J Org Chem 56:6516–6521
18. Alcalde E, Dinares I, Frigola J, Jaime C, Fayet JP, Vertut MC, Miravitlles C, Rins J (1991) Heterocyclic betaines. Aza analogs of sesquifulvalene. 1. Structural studies of 1-alkyl-4-azolylidene-1, 4-dihydropyridines and azolium azolate inner salts. J Org Chem 56:4223–4233
19. Viertorine M, Valkonen J, Pitkänen I, Mathlouthi M, Nurmi J (1999) Crystal and molecular structure of anhydrous betaine, $(CH_3)_3NCH_2CO_2$. J Mol Struct 477:23–29
20. Szafran M, Dega-Szafran Z, Katrusiak A, Buczek G, Głowiak T, Sitkowski J, Stefaniak L (1998) Electrostatic interactions and conformations of zwitterionic pyridinium alkanoates. J Org Chem 63:2898–2908
21. Girreser U, Czyrski A, Hermann TW Synthesis and structure elucidation of a new isoquinolinium inner salt. Tetrahedron Lett 50:4610–4612
22. Barczyński P, Katrusiak A, Dega-Szafran Z, Szafran M (2009) 1-Carboxyethylpyridinium-4-carboxylate inner salt studied by X-ray diffraction, DFT calculations, vibrational and NMR spectroscopy. J Mol Struct 937:85–94
23. Song L, Li HS, Song BD (2006) 1-Carboxymethylpyridinium-2-carboxylate. Acta Cryst E62:o4656–o4657
24. Chen XM, Mak TCW (2009) (1991) Crystal and molecular structure of 3-carboxy-1-(carboxymethyl)pyridinium hydroxide inner salt, $C_5H_4(COO)NCH_2COOH$. J Mol Struct 249:135–140
25. Matsunaga S, Kamimura T, Fusetani N (1998) Isolation of 1-carboxymethylnicotinic acid from the marine sponge Anthosigmella cf. raromicrosclera as a cysteine protease inhibitor. J Nat Prod 61:671–672
26. Barczyński P, Katrusiak A, Koput J, Dega-Szafran Z, Szafran M (2009) Structure of 1-carboxymethylpyridinium-4-carboxylate inner salt studied by X-ray diffraction, DFT calculations, vibrational and NMR spectra. J Mol Struct 933:20–29
27. Bruker (2004) SMART and SAINT. Bruker AXS Inc., Madison, Wisconsin, USA
28. Sheldrick GM (2000) SHELXTL, structure determination Software suite, version 6.14. Bruker AXS, Madison, WI
29. Lynch DE, Thomas LC, Smith G, Byriel KA, Kennard CHL (1998) A new supramolecular synthon using N-methylaniline. The crystal structure of the 1: 1 adduct of N-methylaniline with 5-nitrofuran-2-carboxylic acid. Aust J Chem 51:867–870
30. Smith G, White JM (2001) Short communication: Molecular cocrystals of carboxylic acids: The preparation of the 1: 1 proton-transfer compounds of creatinine with a series of aromatic acids and the crystal structure of that with pyrazine-2,3-dicarboxylic acid. Aust J Chem 54:97–100
31. Lin ZH, Hu KK, Jin SW, Ding AH, Wang YN, Dong LF, Gao XJ, Wang DQ (2017) Crystal and molecular structures of sixteen charge-assisted hydrogen bond-mediated diisopropylammonium salts from different carboxylic acids. J Mol Struct 1146:577–591
32. Aakeröy CB, Fasulo ME, Desper J (2007) Cocrystal or salt does it really matter? Mol Pharm 4:317–322
33. Gao XJ, Jin SW, Jin L, Ye XH, Zheng L, Li JW, Jin BP, Wang DQ (2014) Noncovalent-bonded 1D–3D supramolecular architectures from 2-methylquinoline/quinoline with monocarboxylic acid and dicarboxylic acid. J Mol Struct 1075:384–396
34. Borowiak T, Wolska I, Brycki B, Grzesiak W (2010) Polyamines. IV. Spectroscopic properties of N,N-bis-(1,8-naphthalenedicarboximidopropyl)-N-propylamine and supramolecular interactions in its crystals. J Mol Struct 979:165–171
35. Kaur M, Jasinski JP, Keeley AC, Yathirajana HS, Siddaraju BP (2013) Orphenadrinium dihydrogen citrate. Acta Cryst E 69:o248
36. Nagapandiselvi P, Gopalakrishnan R (2013) Bis(2-hydroxyethyl) ammonium picrate. Acta Cryst E69:o1455
37. Orola L, Veidis MV (2009) Nicotinamide fumaric acid supramolecular cocrystals: diversity of stoichiometry. CrystEngComm 11:415–417
38. Borba A, Albrecht M, Gómez-Zavaglia A, Lapinski L, Nowak MJ, Suhm MA, Fausto R (2008) Dimer formation in nicotinamide and picolinamide in the gas and condensed phases probed by infrared spectroscopy. Phys Chem Chem Phys 10:7010–7021
39. Bakshi PK, Linden A, Vincent BR, Roe SP, Adhikesavalu D, Cameron TS, Knop O (1994) Crystal chemistry of tetraradial species. Part 4. Hydrogen bonding to aromatic π systems: Crystal structures of fifteen tetraphenylborates with organic ammonium cations. Can J Chem 72:1273–1293
40. Bondi A (1964) Van Der Waals volumes and radii. J Phys Chem 68:441–451
41. Spackman MA, Jayatilaka D (2008) Electrostatic potentials mapped on Hirshfeld surfaces provide direct insight into intermolecular interactions in crystals. CrystEngComm 10:377–388
42. Spackman MA, Mckinnon JJ (2002) Fingerprinting intermolecular interactions in molecular crystals. CrystEngComm 4:378–392
43. Mckinnon JJ, Jayatilaka D, Spackman MA (2007) Towards quantitative analysis of intermolecular interactions with Hirshfeld surfaces. Chem Commun 3814–3816